AD-A179 072 ANALYSIS OF WRITE-BEAM-INDUCED DAMAGE ON THE CONDUCTING 1/1
PRIZ (PREOBRASOVA (U) AIR FORCE INST OF TECH
WRIGHT-PATTERSON AFB OH SCHOOL OF ENGI D L ANDERSON
UNCLASSIFIED DEC 86 AFIT/GEP/ENP/86D-1 F/G 7/5 NL

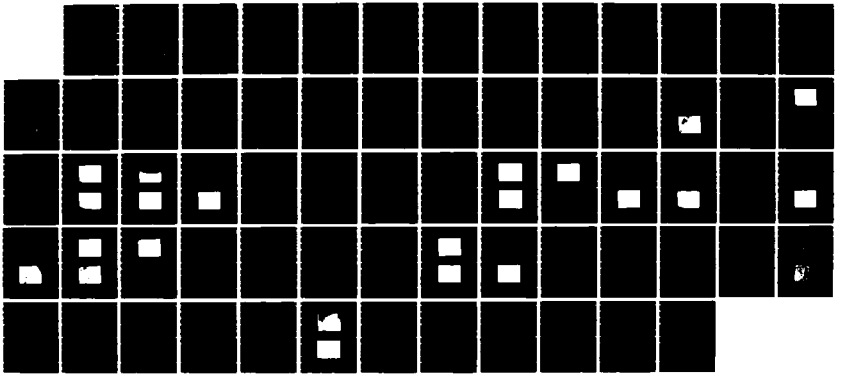

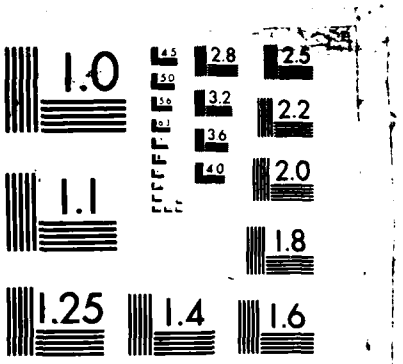

ANALYSIS OF WRITE-BEAM-INDUCED DAMAGE ON THE CONDUCTING PRIZ

THESIS

Danny L. Anderson
First Lieutenant, USAF

AFIT/GEP/ENP/86D-1

DEPARTMENT OF THE AIR FORCE
AIR UNIVERSITY
AIR FORCE INSTITUTE OF TECHNOLOGY

Wright-Patterson Air Force Base, Ohio

AFIT/GEP/ENP/86

ANALYSIS OF WRITE-BEAM-INDUCED DAMAGE ON THE CONDUCTING PRIZ

THESIS

Danny L. Anderson
First Lieutenant, USAF

AFIT/GEP/ENP/86D-1

AFIT/GEP/ENP/86D-1

ANALYSIS OF WRITE-BEAM-INDUCED DAMAGE ON THE CONDUCTING PRIZ

THESIS

Presented to the Faculty of the School of Engineering

of the Air Force Institute of Technology

Air University

In Partial Fulfillment of the

Requirements for the Degree of

Master of Science in Engineering Physics

Danny L. Anderson, B.S.

First Lieutenant, USAF

December 1986

Preface

This thesis is a follow-on to two previous AFIT theses. Both my predecessors reported laser-induced damage to the electrodes of their PRIZ devices. This captured my attention since such damage could significantly reduce the effectiveness of the PRIZ. I felt that if the PRIZ were to be of any practical value to the U. S. Air Force, then its susceptibility to damage should be rigorously studied. As a result of my research, I discovered that the crystal itself was more susceptible to damage than were the electrodes. Upon closer examination of my predecessors' devices, I noticed that their damage was more extensive than they realized and that, in fact, their crystals had received the same type of damage that I observed.

I am very grateful to my advisor, Dr. Theodore Luke, who often answered my questions with more questions. This gave new meaning to the phrase "learning experience". I also want to thank my wife, Mary, and my daughters, Maren and Janna, for their love and support. Their hugs and their smiles nourished and sustained me. But, I dedicate this thesis to my father, Lt. Col. Bobby D. Anderson (deceased).

"Thanks, Dad, for everything."

Danny L. Anderson

Contents

		Page
Preface		ii
List of Figures		v
List of Tables		vii
Abstract		viii
I.	Introduction	1.1
II.	Background	2.1
	Theory of Operation	2.2
III.	Problem Statement	3.1
	Scope	3.1
	Approach	3.2
IV.	Research Report	4.1
	Device Construction	4.1
	Device Identification	4.2
	Experimental Setup	4.3
	Inducing Damage	4.5
	Initial Analysis	4.9
	Controlling Damage	4.13
	Further Analysis	4.19
	Examination of Shields' and Nilius' Devices	4.22
V.	Damage Model	5.1
	Dielectric Breakdown Mechanisms	5.2
	Breakdown Paths	5.4
	BSO Crystal Damage	5.4
VI.	Partial Verification of Damage Model	6.1
VII.	Summary	7.1
	Conclusions	7.1
	Recommendations	7.2

Appendix: Previously Reported Damage A.1

Conical Fracture A.1
Chromium Migration A.1

Bibliography BIB.1

Vita VIT.1

List of Figures

Figure		Page
2.1	Device Mounting	2.1
2.2	Polarization Change Due to Modulated Refractive Indices .	2.3
4.1	Device Mounting	4.1
4.2	Experimental Setup	4.4
4.3	First Signs of Damage - Crystal #1 (Transmitted light @ 100x)	4.6
4.4	Propellor Patterns and Dark Spots - Crystal #2 (Transmitted light @ 125x)	4.8
4.5	Before Removal of Electrode - Crystal #3 (Transmitted light @ 125x)	4.10
4.6	After Removal of Electrode - Crystal #3 (Transmitted light @ 125x)	4.10
4.7	Proximity of Damage to Surface - Crystal #2 (Reflected light @ 450x)	4.11
4.8	Proximity of Damage to Surface - Crystal #2 (Transmitted light @ 450x)	4.11
4.9	Results of Chemical Etching - Crystal #2 (Transmitted light @ 450x)	4.12
4.10	Pits at 2000, 1800, & 1600 Volts - Crystal #4 (Transmitted light @ 110x)	4.17
4.11	Pits at 1400, 1200, & 1000 Volts - Crystal #4 (Transmitted light @ 110x)	4.17
4.12	Pits Induced at 1000 Volts - Crystal #4 (Transmitted @ 320x)	4.18
4.13	Pits Induced at 13000 $\mu W/cm^2$ - Crystal #4 (Transmitted light @ 110x)	4.19
4.14	Cubic-Corner Structure Damage - Crystal #4 (Transmitted light @ 320x)	4.20

4.15 Electrode Damage - Shields' Crystal #S1
(Transmitted light @ 200x) 4.22

4.16 Crack Damage - Shields' Crystal #S2
(Transmitted light @ 200x) 4.23

4.17 Crack Damage and Migration - Nilius' Crystal
(Transmitted light @ 200x) 4.24

4.18 Cubic-Corner Structure - Nilius' Crystal
(Transmitted light @ 200x) 4.24

4.19 Pit Damage - Nilius' Crystal
(Transmitted light @ 200x) 4.25

5.1 Sample of Pit Damage - Crystal #4
(Transmitted light @ 320x) 5.5

5.2 Another Sample of Pit Damage - Crystal #4
(Dark-field reflected light @ 320x) 5.5

5.3 Sample of Crack Damage - Crystal #4
(Transmitted light @ 320x) 5.6

6.1 Smooth/Shiney Surface after 13 Second Etch - Crystal #5
(Transmitted light @ 320x) 6.2

6.2 Dull/Rough Surface after 13 Second Etch - Crystal #5
(Transmitted light @ 320x) 6.2

A.1 Conical Fracture - Shields' Crystal #S1
(Transmitted light @ 35x) A.2

A.2 Chromium Migration - Shields' Crystal #S1
(Transmitted light @ 200x) A.2

List of Tables

Table		Page
4.1	Comparison of PRIZ Devices Studied	4.2
4.2	Results of Attempts to Induce Damage	4.5
4.3	Results of Attempts to Control Damage on Crystal #4 (Varying the Applied Field Voltage.)	4.14
4.4	Results of Attempts to Control Damage on Crystal #4 (Varying the Write-Beam Irradiance.)	4.15
4.5	Results of Electrode Reversal on Crystal #4	4.20

Abstract

The susceptibility of the conducting PRIZ to write-beam-induced damage was studied. Using a HeCd laser as a write-beam, damage was intentionally induced on PRIZ devices. Careful examination of the devices revealed essentially four types of damage: "electrode damage", "pit damage", "striation", and "crack damage". Striation may have been a pattern of overlapping less severe crack damage.

The write-beam irradiance and applied E-field strength were varied in search of damage thresholds, and analysis was performed to discover the location and nature of the damage. Electrode damage was in the form of either evaporation or migration.

Pit damage, striation, and crack damage were related: all occurred in the "high-field" region of the PRIZ, i.e. near the negative surface; all displayed a symmetric structure resembling the corner of a cube (pits displayed this structure only after chemical etching); and, although striation and cracks did not always appear with pit damage, pits always accompanied striation and crack damage.

On one surface of a crystal, dense patches of pits and striation were induced, while on the other surface, crack damage and fewer pits resulted. This was found to be due to a difference in the surface imperfections caused by the mechanical preparation of the crystals.

Devices used in earlier AFIT research, by Duncan Shields and Mark Nilius, were examined and found to have similar damage. This damage had previously eluded detection.

ANALYSIS OF WRITE-BEAM-INDUCED DAMAGE ON THE CONDUCTING PRIZ

I. Introduction

The PRIZ, an acronym for Preobrasovatel Izobrazheniya (Image Transducer) is a Soviet designed spatial light modulator (14:1). The device consists of a photorefractive crystal in which, under the influence of an applied longitudinal E-field, the refractive indices are modulated by the transverse electro-optic effect.

The device can operate in one of several modes. In the "dynamic image selection" mode, the device ignores all but the moving portions of an image. This feature suggests the possibility of using the device as a moving target indicator. This project was designed to study the device's susceptibility to write-beam-induced damage. The possibility of the write-beam inducing damage to the PRIZ merited exploration, since any damage could severely degrade the operation of the device.

As a result of this research project, damage was found to be easily induced on the PRIZ, at write-beam irradiance levels well below those required to operate the device in the dynamic image selection mode. The damages observed were labeled "electrode damage", "pit damage", "striation", and "crack damage". Pit damage, striation, and crack damage occurred in the crystal and displayed a symmetric structure dubbed "cubic-corner structure" in this report. Striation and

crack damage may, in fact, have been different degrees of the same type of damage, i.e. striation may have been a pattern of overlapping less severe crack damage.

This report details the conditions under which the write-beam caused damage, and characterizes the damage encountered. Careful examination of earlier AFIT PRIZ devices revealed similar damage, which had eluded prior detection. Also, evidence is presented which indicates that the damage is related to surface disorder caused by mechanical preparation of the material, e.g. sawing, grinding, and lapping.

II. Background

There are two versions of the PRIZ device which, since they are constructed differently, exhibit different properties (8:1). The "conducting" version of the PRIZ consists of a thin wafer of Bismuth Silicon Oxide (BSO), cut such that the large faces correspond to the (111) crystal planes. Transparent electrodes, e.g. platinum or chromium, are vacuum deposited on these faces (see figure 2.1). The "standard" version of the PRIZ has a thin dielectric layer between the crystal surfaces and the electrodes. The conducting PRIZ, because it lacks this layer, exhibits properties which lend themselves to several practical applications of interest to the U. S. Air Force. One application of particular interest is that of a moving target indicator.

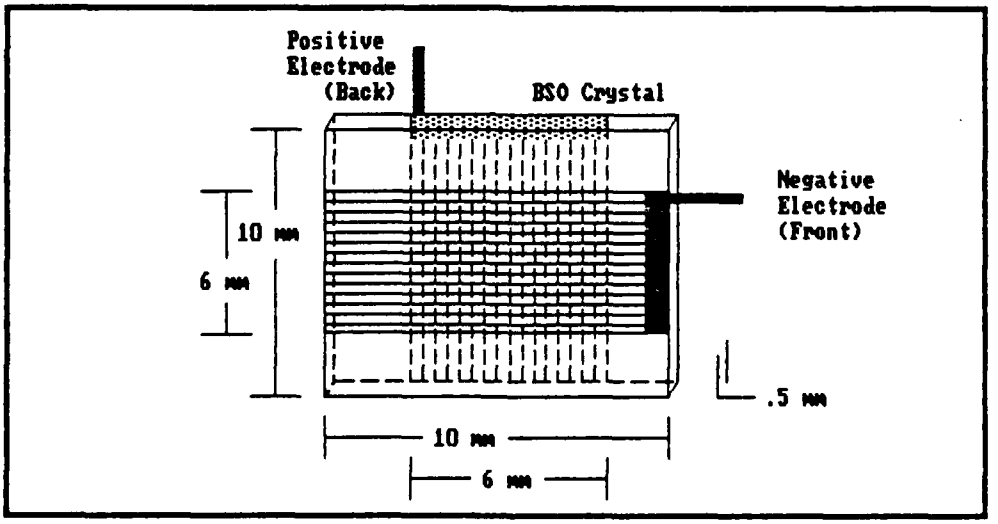

Figure 2.1. PRIZ Device.

The conducting PRIZ serves such a function when it is operated in what is known as the "dynamic image selection" mode. Only the conducting version was considered in this research project. To date, the only successful non-Soviet fabrication of a conducting PRIZ has been reported at the Air Force Institute of Technology, first by Shields (8), and subsequently by Nilius (14).

Theory of Operation

The device works on the principle of photorefraction, i.e. light induced changes in the refractive indices via the transverse electro-optic effect. A longitudinal field is established by the application of a d.c. voltage between the electrodes, with the negative electrode on the "front", or illuminated, surface. The crystal is then illuminated from the front with a write-beam of suitable wavelength (not necessarily coherent). Donors are excited from deep donor centers and drift, under the influence of the applied E-field, until they are trapped at trap centers. (Donor centers have been identified as silicon vacancies, and the trap centers as luminescence centers (14:10).) The donors may, at this point, be thermally detrapped or optically reexcited and drift to another trap center. Thermal detrapping is a very slow process. The resulting space-charge field spatially modulates the refractive indices in the illuminated region of the crystal, via the electro-optic effect. The induced birefringence, in turn, affects the polarization of light passing through that region (14:8-9).

When the crystal is illuminated from the front with a coherent, second beam, the modulated indices are "read". This read-beam must be

of wavelength such that excitation of donors due to this beam is minimal. The PRIZ is located between two polarizers which, after accounting for the optical activity of the crystal itself, are effectively crossed. Thus, the read-beam will not pass the second polarizer, or analyzer, except where the index of refraction in the crystal has been modulated by the write-beam, causing the polarization to change (see figure 2.2). The amplitude of the coherent read-beam, then, after passing the crossed polarizers, is related to the intensity of the original input image (8:8). A filter, which passes the read-beam wavelength, removes all other wavelengths, including that of the write-beam, from the final image.

The applied field is not longitudinally uniform across the device in illuminated regions. There is a high-field region or layer near the negative electrode surface of the device. This region extends from the

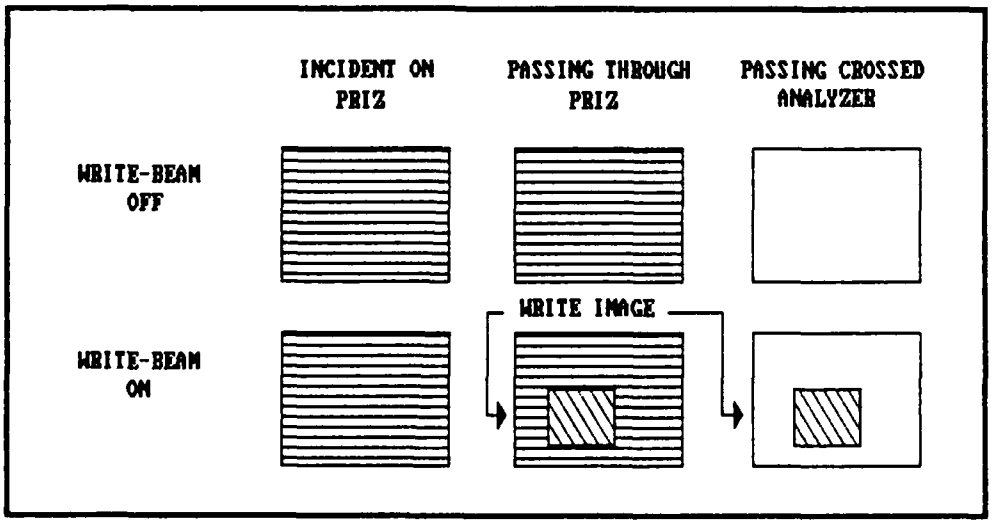

Figure 2.2. Polarization Change Due to Modulated Refractive Indices. (Lines indicate the direction of polarization.)

surface to a depth of about 30 to 100 μm (11:161). The damage observed during this project was consistently found within this region, i.e. on the surface and extending to a depth roughly equal to that of the high-field region.

In one mode of operation, the device is capable of ignoring the constant or nonvarying portion of an image, and modulating the read-beam with only the time varying, or moving, portion. This mode is known as the "dynamic image selection" mode, and in it the device acts essentially as a moving target indicator. Whether or not the device operates in this mode depends on the write-beam energy density; higher energy densities result in shorter memory times. Nilius reported that energy densities much greater than 50 $\mu J/cm^2$ are required for dynamic image selection operation (8:31). While the write-beam was characterized in terms of irradiance (power density) in this project, the fact that the device did not operate in the dynamic image selection mode indicated that the damage was occurring at energy-densities less than those required for that mode.

III. Problem Statement

The practical value and effectiveness of a device such as the PRIZ is, of course, quite dependent upon its durability. Damage to either the electrodes or the crystal could reduce the operating effectiveness of the device. In practical use, depending upon the operating environment and the application, damage to the crystal may or may not be a real threat. However, it has been shown that under some conditions, such as writing directly to the device with a focused laser spot, the threat of damage does exist. Damage reported to date is summarized in an appendix.

Scope

The goal of this thesis project was to discover and report as much as possible about the potential for write-beam-induced damage to the PRIZ device. Damage was induced at write-beam energy densities less than those required for dynamic image selection mode (irradiances are reported). The read-beam irradiance was held constant and, although the read-beam may have contributed to damage, it was not observed to induce damage by itself; therefore, research was limited to the affects of the write-beam. The longitudinal field strength, however, was found to have some influence on damage susceptibility.

Approach

Presupposing that damage could be intentionally induced, the following questions were posed as a guide to research efforts.

1. Under what conditions does damage occur?
2. Is the damage repeatable?
3. Is the damage in the electrode or the crystal?
4. If in the crystal, how far is it from a surface? Which surface?
5. Is there any structure to the damage?
6. What caused the damage?

Several experiments were performed in an attempt to quantify and/or qualify the PRIZ device's susceptibility to damage. The first step was to verify that damage could, in fact, be induced on the crystal or the electrodes. Initially, high write-beam irradiances and field strengths were used to intentionally cause damage. The field and the irradiance were then decreased in attempts to induce damage at more practical working levels for the device.

Once achieved, initial analysis was performed on the damage. The devices were carefully scrutinized under a microscope using transmitted, bright-field reflected, and dark-field reflected (oblique) light, with magnifications ranging from 35x to 450x. In order to search for structure, chemical etching was employed to enhance the damage. Video recordings of the PRIZ output were maintained throughout the experiments in order to attempt to correlate damage with visible responses.

Damage was then induced under controlled conditions. The write-beam irradiance and the applied longitudinal field strength were varied to determine their influence on damage susceptibility and to establish approximate damage thresholds. Attempting to cause damage with the electrodes reversed brought additional valuable information to light.

IV. Research Report

Four types of damage were discovered and, after analysis, labeled "electrode damage", "pit damage", "striation", and "crack damage". The striation, or sets of fine, parallel lines, seemed to be less severe manifestations of overlapping crack damage. This section describes the experimental and analytical procedures, and the results of both.

Device Construction

Thin, transparent platinum electrodes were vacuumed deposited on the (111) faces of each crystal. The crystals were then mounted on plexi-glass slides with a hole, slightly smaller than the crystal, cut in the center (see figure 4.1). The crystals were attached to the slides with a small drop of silver paint. (Paint was used, as opposed

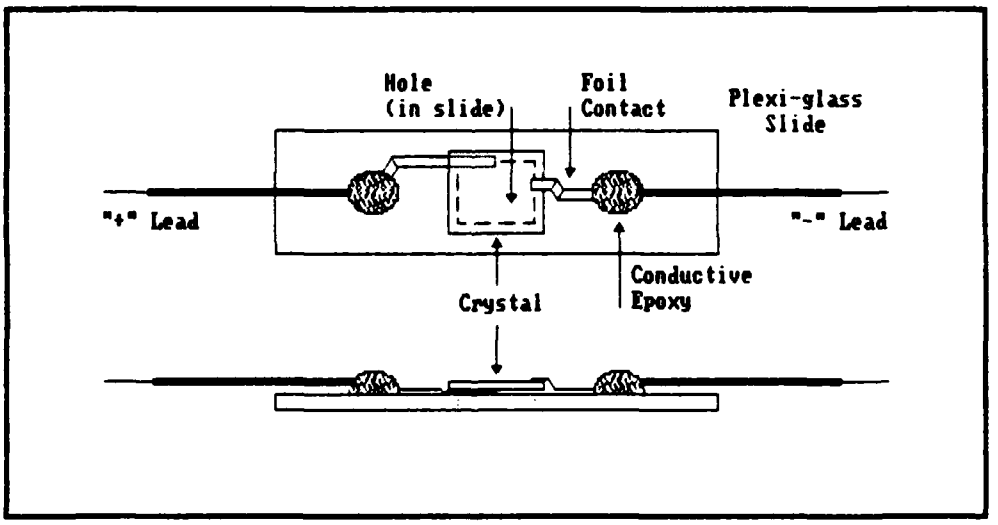

Figure 4.1. Device Mounting.

to epoxy, to facilitate removal of the crystals.) A narrow strip of aluminum foil was attached to each electrode with the conductive paint. The opposite ends of the foil strips were then attached to wires which had been cemented to the slide with a conductive epoxy.

Device Identification

Eight PRIZ devices were used during this research project. Two devices used by Shields and another used by Nilius were still available for examination. Five additional BSO crystals were acquired. The major differences between the devices were manufacturer and electrode material. Table 4.1 compares the eight devices.

TABLE 4.1

Comparison of PRIZ Devices Studied

Researcher	Electrode	Manufacturer	Device Reference
Shields	Chromium	Crystal Tech.	Shields' crystal #S1
Shields	Chromium	Crystal Tech.	Shields' crystal #S2
Nilius	Chromium	Sumitomo Elec.	Nilius' crystal
Anderson	Platinum	Sumitomo Elec.	Crystal #1
Anderson	Platinum	Sumitomo Elec.	Crystal #2
Anderson	Platinum	Sumitomo Elec.	Crystal #3
Anderson	Platinum	Sumitomo Elec.	Crystal #4
Anderson	None	Sumitomo Elec.	Crystal #5

Experimental Setup

The experimental setup to operate the PRIZ device, and to attempt to induce damage, is shown in figure 4.2. Each piece of equipment in the figure is labeled with a letter and a number. The letter identifies the piece with a particular path, as follows:

W: Write-beam path
R: Read-beam path
I: Imaging/optical path
E: Electrical path

The shutters (R2 & W2) served to control the beam on/off status so that it was not necessary to go through time-consuming "power-up" or "power-down" procedures with the lasers. The apertures (R6 & W7) and the neutral density filters (R3 & W4) controlled the irradiance of the beams. The lens (W6) focused the write-beam such that the beam waist was on the surface of the PRIZ (I1), while a steerable mirror (W8) provided for horizontal and vertical movement of the write-beam across the PRIZ. A prism (W9) redirected the write-beam onto the PRIZ at nearly normal incidence (nearly parallel to the read-beam). The polarizer (R4) in the read-beam path was not necessary since the laser output was already nearly completely polarized. It served, however, to ensure complete polarization and to control the direction of that polarization. The microscope (I2) magnified the image from the PRIZ for viewing with video equipment. The filter (I3), which passes the read-beam wavelength, prevented all other wavelengths, including that of the write-beam, from entering the video camera. A resistor (E6) was used to limit the current passing through the PRIZ. The video equipment (I4, I5, & I6) allowed monitoring/recording of the visual output, while the ammeter and oscilloscope displayed the current.

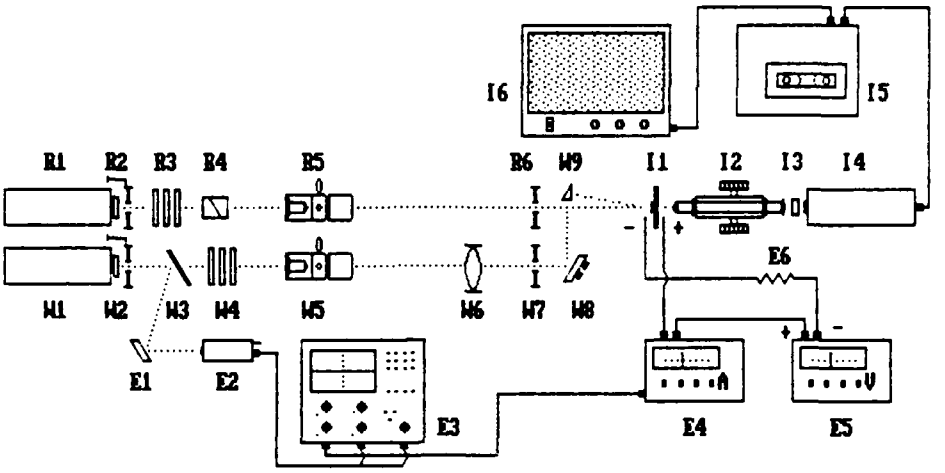

W1: Write-beam source (3 mW, CW, HeCd laser, at 442 nm)
W2: Shutter
W3: Beam splitter (microscope slide)
W4: Neutral density filters
W5: Jodon beam expander, spatial filter, and collimator
W6: Lens (500 mm focal length)
W7: Aperture
W8: Steerable mirror
W9: Prism

R1: Read-beam source (1 mW, CW, HeNe laser, at 632.8 nm)
R2: Shutter
R3: Neutral density filters
R4: Polarizer
R5: Jodon beam expander, spatial filter, and collimator
R6: Aperture

I1: PRIZ device
I2: Microscope (5.6x objective, analyzer, 10x eyepiece)
I3: Filter (632.8 nm)
I4: Video camera
I5: Video recorder
I6: Video monitor

E1: Mirror
E2: FND-100 detector
E3: Oscilloscope
E4: Ammeter
E5: High-voltage power supply
E6: Resistor (30 MΩ)

Figure 4.2. Experimental Setup.

Inducing Damage

Initially, in order to verify that damage could be induced, the voltage was set at 2000 V, with the negative electrode on the front surface of the device. The device was operated by applying this field across the electrodes, writing an image to the device, and simultaneously reading the image. A HeNe laser (λ = 632.8 nm) provided the read-beam. A constant irradiance of 100 $\pm$ 10 $\mu W/cm^2$ was used throughout this project. The image employed was merely the focused spot (70 $\pm$ 10 μm in diameter), from a HeCd laser (λ = 442 nm), which was scanned horizontally and vertically across the device.

Three crystals, or PRIZ devices, were initially used to verify that damage could be induced, not only at high irradiances (crystal #1), but also at reasonable operating levels (crystals #2 and #3). Damage was then induced on a fourth crystal, under carefully controlled conditions, for further analysis. The results of the initial damage attempts (crystals #1, #2, and #3) are summarized in table 4.2.

TABLE 4.2

Results of Attempts to Induce Damage.

Crys.	Write-beam Irradiance	Damage Results	Time
#1	38.2 W/cm^2	Trails of pits on surface, and overlapping striation	Instantaneous
#2	2.93 mw/cm^2	Propellor pattern cracks just under surface, and scattered pits	Instantaneous
#3	293 $\mu W/cm^2$	Propellor pattern cracks just under surface, and scattered pits	After 3 seconds

In each case, in table 4.2, the E-field was held at 2000 V, and damage occurred on the negative electrode side of crystal (in the high-field region). A high write-beam irradiance (~ 38.2 W/cm^2) was applied to crystal #1 to ensure a high probability of damage. To avoid conical fracture (see appendix), due to such a high irradiance, the write-beam was not left idle in one location, and the current was limited by the 30 MΩ resistor (E6). Upon write-beam illumination, visible arcing occurred, emanating from the foil contact on the front surface of the PRIZ and extending to the location of the write-beam spot, or image. As the write-beam was scanned across the device, the arcing followed.

Microscopic examination of the crystal revealed two forms of damage: lighter trails, found on both the front and back surfaces, and trails of dark spots (see figure 4.3), found only on the front. The

Figure 4.3. First Signs of Damage - Crystal #1 (Transmitted light @ 100x).

light trails were found across the entire crystal, but were more concentrated near the foil contacts. The trails of dark spots, on the other hand, being horizontal and vertical, appeared to correspond to the paths "travelled" by the write-beam. A large number of the spots showed signs of striation emanating from them. The striae were overlapping patterns of one to three thin lines extending from each spot, with any two lines 120 degrees apart and always oriented in the same direction. In other words, in cases where three lines emanated from a spot, the striae resembled a three-bladed propellor, or the corner of a cube. In other cases, only one or two striae emanated from a spot, though always parallel to striae in the three-bladed pattern. This suggested a correlation with the macroscopic structure of the crystal.

For crystal #2, the irradiance was lowered to 2.93 mW/cm^2, and no arcing occurred. However, when the write-beam was scanned slowly (rate unknown), short, narrow, bright lines appeared on the video monitor, extending outward from the written line image (i.e. where the write-beam had passed). Passing the write-beam across the bright lines again caused them to spread, or lengthen. When the over-head flourescent lights (at an irradiance of 2 μW/cm^2) were turned on, while the 2000 V field was applied and the write-beam off, the lines lengthened considerably and, in some cases, met other lines. Attempts to repeat this flourescent light effect later, with crystal #4, failed.

Under the microscope, damage was found to have occurred on the front surface, in the form of spots, like those on crystal #1, and lines, resembling scratches or cracks (see figure 4.4). These lines

Figure 4.4. Propellor Patterns and Dark Spots - Crystal #2 (Transmitted light @ 125x).

were much longer and wider than the striae observed among spots on crystal #1. They still displayed the same symmetric pattern (the three-bladed propellor) observed amoung the striation of crystal #1; however, they were far fewer in number and density (i.e. there was no overlapping). This "propellor pattern" was most obvious near the intersection of three lines. (Although the striation displayed a similar pattern, the term "propellor pattern" will refer to the larger, more sparse, non-overlapping patterns first observed on crystal #2.) Farther from the intersection, the lines often curved toward or away from each other. A dark spot was located at the center, or intersection, of propellor patterns and, in some cases, dark spots were found on the outward-extending lines.

Attempts were made to cause propellor patterns in regions of spot damage. After several attempts, in different locations, a propellor pattern was created with an existing dark spot at the center. The lines of the structure curved towards other existing dark spots. However, in another attempt, at a spot-free location, a propellor pattern was created, exhibiting new dark spots at its center and on its lines.

The irradiance of the write-beam was lowered to 293 $\mu W/cm^2$ before using crystal #3. Initially, no damage visibly occurred on the monitor as the write-beam scanned. However, when the write-beam was left idle for more than 3 seconds, at a random location, damage occurred at that location. Microscopic examination revealed the same damage found on crystal #2, i.e. scattered dark spots and propellor patterns, on the front surface. Once again, re-illuminating propellor patterns caused the lines to spread outward.

Initial Analysis

Polishing the platinum electrodes off crystals #1 and #3 removed the lighter regions. Thus, the damage was electrode degradation, possibly migration or evaporation. The propellor patterns and the dark spots remained and, therefore, were located in, or on, the crystal itself (compare figures 4.5 & 4.6).

Varying the focus on the microscope revealed that there was some depth to both the dark spots and the lines, i.e. they were not just on the surface. Yet focusing through the crystal onto the back surface revealed no damage, indicating that the spots and lines did not extend completely through the crystal. When the spots and propellor patterns

Figure 4.5. Before Removal of Electrode - Crystal #3 (Transmitted light @ 125x).

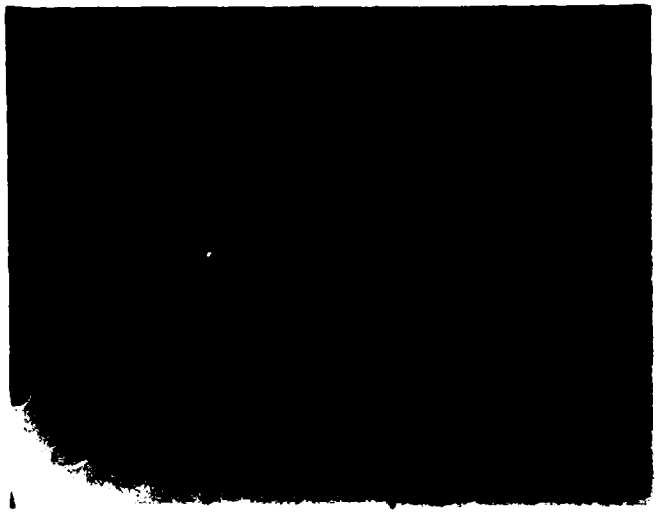

Figure 4.6. After Removal of Electrode - Crystal #3 (Transmitted light @ 125x).

Figure 4.7. Proximity of Damage to Surface - Crystal #2 (Reflected light @ 450x).

Figure 4.8. Proximity of Damage to Surface - Crystal #2 (Transmitted light @ 450x).

were observed with reflected, versus transmitted, light, the spots were clearly visible, but the lines were barely discernable (compare figures 4.7 & 4.8). The spots appeared to be smooth and rounded at the bottom. Therefore, the spots were pits which began at the surface and extended slightly into the crystal, while the lines appeared to be cracks just below the surface. Viewing the propellor pattern lines from the edge of a broken piece of crystal #2 verified that the lines were cracks beginning at or immediately below the surface and extending normal to the surface to a depth of approximately 1/10 to 1/7 of the thickness of the crystal (i.e. ~ .044 to .063 mm deep). Striation was barely visible under reflected light, and was, therefore, located on or just under the surface, though having no noticeable depth.

Chemical etching (6:2746-2748) was performed on damaged samples to enhance the damage (see figure 4.9). This revealed that even pits

Figure 4.9. Results of Chemical Etching - Crystal #2 (Transmitted light @ 450x).

which were not visibly associated with striation or propellor patterns possessed that same symmetric cubic-corner structure, related to the crystallographic structure of the crystal.

In summary, as a result of initial damage attempts, four types of damage occurred: electrode damage, pit damage, striation, and crack damage. The electrode damage occurred only at an extremely high irradiance, and was not the subject of further research. Pit damage, striation, and crack damage, on the other hand, occurred in the crystal and displayed a cubic-corner structure related to the cubic structure of the BSO crystal and following the crystallographic directions. It was not completely certain whether the cracks and striation were related to each other, since the size and depth differed; however, since both displayed cubic-corner structure, the propellor patterns, in which the lines were found to be cracks, may have been merely more advanced stages of striation. The difference in the density of the patterns for each case (dense, overlapping striation vs. sparse propellor patterns) was unexplainable at this stage.

Controlling Damage

Having obtained damage, attempts to induce damage under controlled conditions were made on crystal #4. The E-field and the write-beam irradiance were varied through predetermined ranges, and the resultant damages were compared.

Initially, the irradiance of the write-beam was held constant (at 325 $\pm$ 50 $\mu W/cm^2$), while the E-field was varied between 1000 and 2000 V, in increments of 200 V. The results are summarized in table 4.3.

TABLE 4.3

Results of Attempts to Control Damage on Crystal #4.
(Varying the Applied Field Voltage.)

Applied Field Voltage (V)	Damage Result	Visibiliy	Success Rate
2000	Dense patches of pits, and overlapping striation	Excellent	4 out of 4
1800	Dense patches of pits, and overlapping striation	Excellent	4 out of 4
1600	Less dense patches of pits, and overlapping striation	Fair	3 out of 4
1400	Sparse patches of pits	Poor	2 out of 4
1200	Very sparse patches of pits	Very Poor	2 out of 4
1000	A few pits	Nearly invisible	1 out of 4

Then, holding the voltage constant (at 2000 V), the irradiance was varied by changing the optical density of the neutral density filters in the write-beam path. The irradiances were approximately 100, 300, 1000, 4000, and 13000 $\mu W/cm^2$. The results are summarized in table 4.4. Rather than scanning the write-beam, it was left idle at four different targeted locations, for each of the eleven combinations of conditions. Illumination time at each location was arbitrarily selected to be 30 seconds since, in practicle applications, long dwell times are a possibility.

TABLE 4.4

Results of Attempts to Control Damage on Crystal #4.
(Varying the Write-Beam Irradiance.)

Write-Beam Irradiance ($\mu W/cm^2$)	Damage Result	Visibiliy	Success Rate
13000	Dense patches of pits, and overlapping striation, with trails of pits between patches	Excellent	4 out of 4
4000	Dense patches of pits, and overlapping striation	Excellent	3 out of 4
1000	Dense patches of pits, and overlapping striation	Excellent	3 out of 4
300	Dense patches of pits, and overlapping striation	Excellent	3 out of 4
100	Very sparse patches of pits	Poor	2 out of 4

During these attempts, no crack damage occurred (unless striation is a manifestation of cracking); however, pit damage was repeatedly, though not consistently, induced. Again, the damage was found only on the front, or illuminated, surface (i.e. the negative electrode side). At some random locations, the write-beam spot, or image, self-erased in less than 3 seconds, and no damage occurred. Damage was successfully induced when the image did not self-erase. In those cases, at some time between 3 and 20 seconds, an irregular (i.e. not periodic) flicker

was observed, indicating that damage had occurred or was occurring. Although the probability of damage was linked to location on the crystal, in that at some locations damage could not be induced at a given irradiance, increasing the irradiance increased the probability of damage at any given location.

The pits occurred in patches, or circular regions, which were approximately 70 μm in diameter. Interestingly, this was roughly the diameter of the write-beam spot on the PRIZ surface. Striation was, again, clearly visible among the pits.

Decreasing the applied voltage in increments, from 2000 to 1000 V, decreased the visibility of the patches of pits in four ways (see figures 4.10 & 4.11). First, the diameter of the patches was slightly reduced; second, the density of pits in each patch was reduced; third, the visibility of the individual pits was reduced, due to decreases in their diameter and depth; and fourth, visibility of the striation was reduced. At 2000 and 1800 V (regions A and B, respectively, in 4.10), the pits were quite visible, and the striation clearly displayed cubic-corner structure. At 1600, 1400, and 1200 V (region C in 4.10, and regions D and E in 4.11, respectively), the patches were detectable, though with difficulty, under transmitted light. At 1000 V (region F in 4.11), as seen at a magnification of 110x, the damage was completely invisible under transmitted light, and only barely detectable under dark-field reflected light, i.e. the pits were so small that only scattering from oblique incident light revealed their presence.

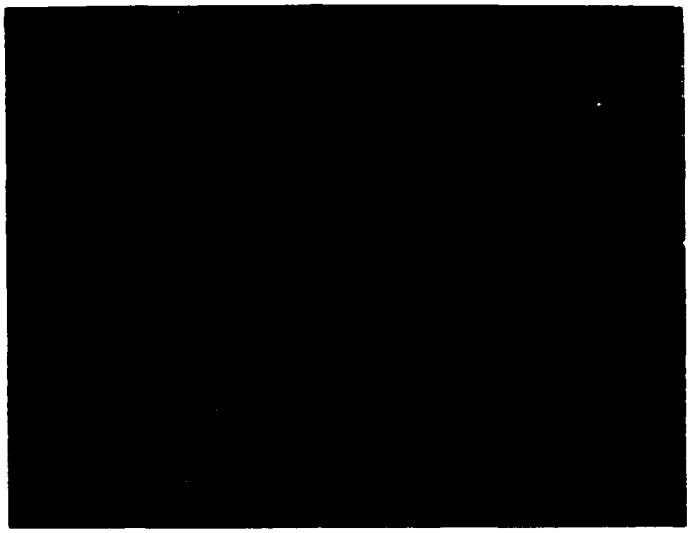

Figure 4.10. Pits at 2000, 1800 & 1600 Volts - Crystal #4
(Transmitted light @ 110x).

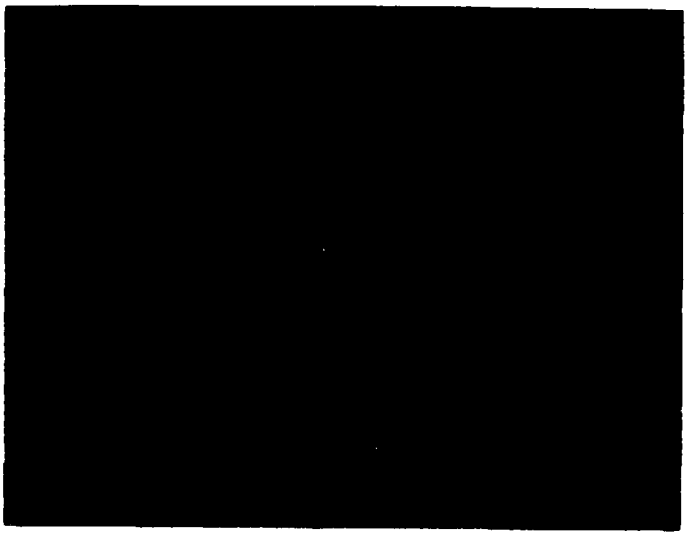

Figure 4.11. Pits at 1:00, 1200, & 1000 Volts - Crystal #4
(Transmitted light @ 110x).

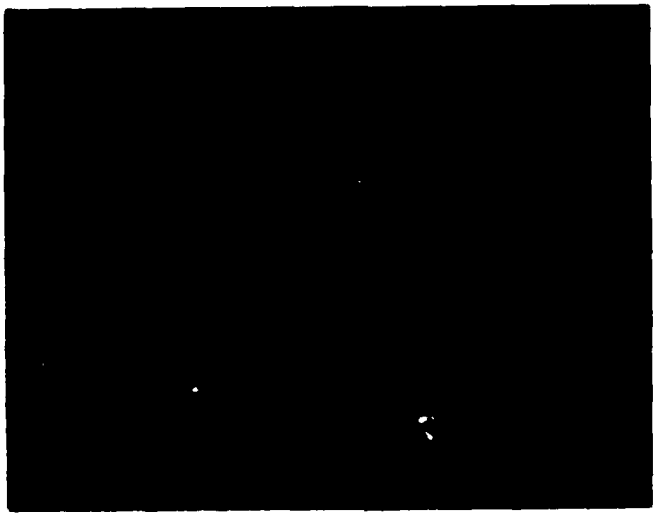

Figure 4.12. Pits Induced at 1000 Volts - Crystal #4 (Transmitted light @ 320x).

A closer look (320x), verified that pits were present (see figure 4.12).

Decreasing the voltage also decreased the probability of damage occuring: at 2000 and 1800 V, four out of four damage attempts were successful; at 1600 V, three out of four were successful; at 1400 and 1200 V, two out of four were successful; and at 1000 V, only one out of four was successful.

Varying the irradiance also affected damage visibility and the probability of occurrence. Patches of pit damage obtained at 300, 1000, and 4000 $\mu W/cm^2$ showed no significant differences. At these irradiances, damage occurred in three out of four attempts, and pit

densities were roughly the same. At 100 μW/cm², however, the density of pits was considerably reduced, and damage occurred in only two out of four attempts. On the other hand, at 13000 μW/cm², damage occurred in four out of four attempts, and dense trails of pits occurred between very dense patches (see figure 4.13). The trails corresponded to the motion of the write-beam spot as it moved from one targeted location to another.

Further Analysis

The obvious question, at this stage, was "Why did pit damage occur on all four crystals, while crack damage occurred on only two?" Reversing the electrodes (i.e. negative on the back) on crystal #4 provided a possible answer. Labeling the original front surface of crystal #4 (containing the pit damage) as "A", and the opposite surface as "B",

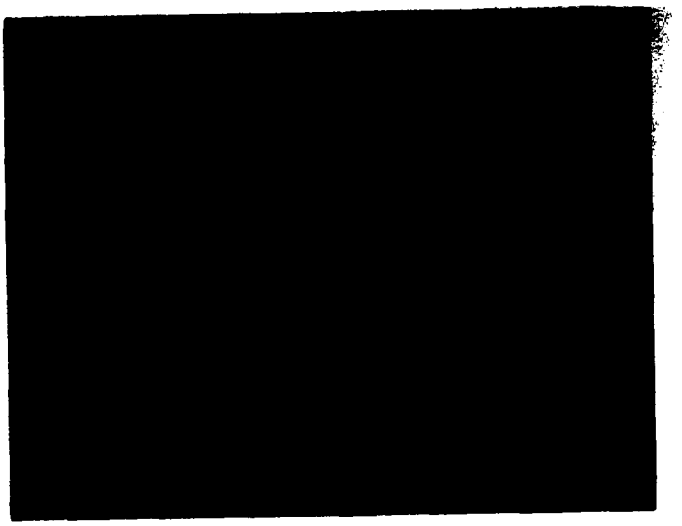

Figure 4.13. Pits Induced at 13000 μW/cm² - Crystal #4 (Transmitted light @ 110x).

TABLE 4.5

Results of Electrode Reversal on Crystal #4.

Illuminated Surface (Front)	High-Field Surface (Neg.)	Damage Result
A	B	Crack damage on back (side B)
B	B	Crack damage on front (side B)
B	A	Pit damage on back (side A)

damage was attempted under three negative electrode/illuminated surface combinations. The results are summarized in table 4.5.

With a 2000 V applied field and an irradiance of approximately 3000 $\mu W/cm^2$, propellor patterns (crack damage) occurred for the first time on crystal #4 (see figure 4.14). Once again, the damage

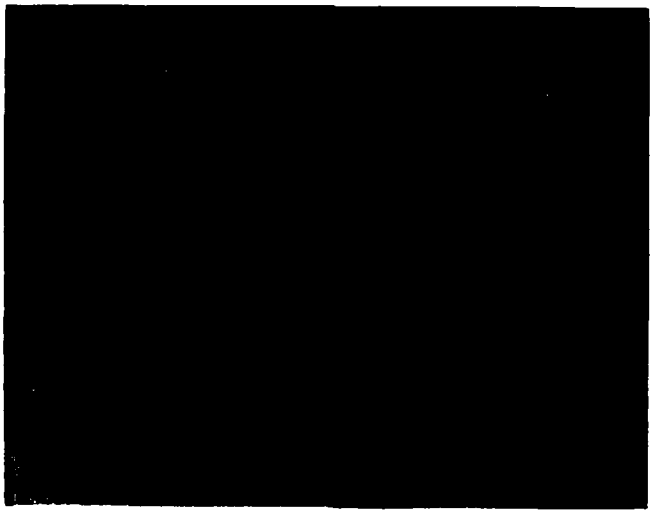

Figure 4.14. Cubic-Corner Structure Damage - Crystal #4 (Transmitted light @ 320x).

occurred on the negative (now the back) surface (side B), i.e. near the high-field region. Varying the irradiance, further attempts to induce crack damage were made. Irradiances of 200 and 600 $\mu W/cm^2$, also resulted in crack damage, though, once again, damage could not be induced at every location on the crystal. No damage occurred at 100 $\mu W/cm^2$.

Next, the crystal was reversed such that the back surface (side B) had become the front surface, and the electrodes were restored such that the negative electrode was again on the front (side B), or illuminated, surface. Damage attempts resulted in more cracks on the front.

Then, the electrodes were reversed, so that the negative electrode was again on the back (side A). The result was a patch of pit damage on that surface. Therefore, damage only occurred on the negative, or high-field, side of the crystal, with cracks and scattered pits occurring on one side, and dense patches of pits and striation occurring on the other.

As a result of this further analysis, the following conclusions were drawn. Damage to the BSO crystal occurred when the applied longitudinal E-field was between 1000 and 2000 V, and when the irradiance of the write-beam was some value greater than 100 $\mu W/cm^2$, depending on the E-field. The damage was repeatable, though not consistent, i.e. at a given irradiance, damage could not be induced at every location attempted; however, increasing the irradiance increased the probability of damage occuring at a given location. The damage occurred in the form of pits, striation, and cracks, on and just under the surface, to a depth of approximately 1/7 the thickness of the crystal (roughly that of the

high-field region). Each displayed a similar symmetric structure, resembling the view of the corner of a cube.

Examination of Shields' and Nilius' Crystals

It was curious that such damage, so easily induced, had not been observed before. Was this the first time such damage had occurred, or had it, perhaps, occurred before and gone unnoticed? Careful examination of crystals used by Shields and Nilius revealed similar damage encountered during this research project, i.e. electrode damage, crack damage, striation, and pit damage, in addition to the damage that they observed and reported.

Shields' crystal #S1 revealed electrode damage in the chromium migration region (see figure 4.15). This seemed to hint that electrode damage might have been early stages of migration. On the other hand,

Figure 4.15. Electrode Damage - Shields' Crystal #S1 (Transmitted light @ 200x).

this damage might have been evidence of electrode evaporation, completely unrelated to migration.

Some crack damage was found on Shields' crystal #S2 (see figure 4.16). Nilius' crystal also revealed crack damage, though far more extensive than Shields'. In many cases, the migration damage, which Nilius did notice, emanated from and/or was encompassed by crack damage (see figure 4.17). Obvious manifestations of cubic-corner structure were also found (see figure 4.18).

Pit damage was also observed on both Nilius' crystal and Shields' crystal #S2. On Shields' crystal the pits were few in number and scattered in the vicinity of the crack damage. On Nilius' crystal, though, the pits appeared in patches, or in trails (see figure 4.19).

Figure 4.16. Crack Damage - Shields' Crystal #S2 (Transmitted light @ 200x).

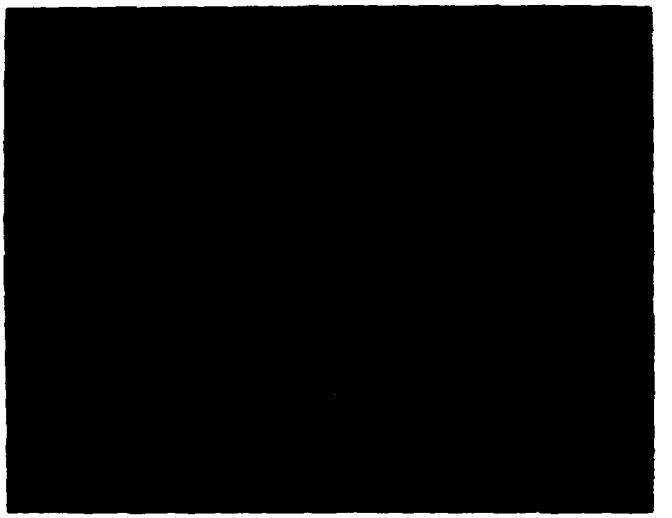

Figure 4.17. Crack Damage and Migration - Nilius' Crystal (Transmitted light @ 200x).

Figure 4.18. Cubic-Corner Structure - Nilius' Crystal (Transmitted light @ 200x).

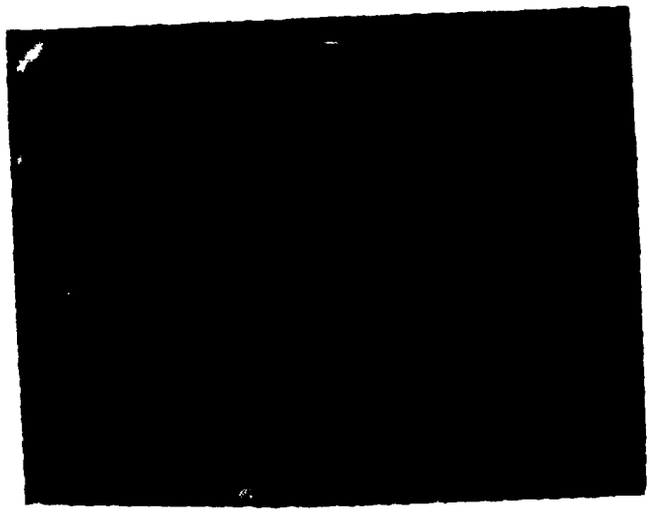

Figure 4.19. Pit Damage - Nilius' Crystal (Transmitted light @ 200x).

V. Damage Model

At this point, five of the six questions posed in the problem statement have been answered; however, new questions have arisen. The five questions which will be considered in the following pages are:

1. What causes the damage?
2. Why does the damage take on the form and structure that it does?
3. Why does the damage only occur at certain locations?
4. Are cracks and striae related?
5. Why do cracks occur on one surface, while striae occur on the other, associated with denser patches of pits?

The answers to these questions, which can only be hypothesized, are based upon the theory and mechanisms of dielectric breakdown, and upon the damage analysis performed during this project.

The BSO crystal is wide band gap photoconductor. Shields describes the material as follows:

> BSO is a sillenite compound that is grown in single crystal boules by the Czochralski technique. The crystals exhibit zincblende structure and belong to the 23 cubic symmetry point group. BSO is a para-electric electrooptic photoconductive material with high resistivity. BSO is also optically active (14:7-8).

That the crystal basically behaves as a dielectric until photoexcitation occurs, is not sufficient justification for applying principles of dielectric breakdown to an analysis of the damage induced. However, add to that the fact that damage observed during this project strongly resembles published descriptions of dielectric breakdown (1,5,11,13,16, & 17), and it becomes apparent that dielectric breakdown, or similar processes, are involved. (Shields attributed a conical fracture induced on one of his devices to dielectric breakdown (see appendix).)

Dielectric Breakdown Mechanisms

There are several mechanisms which can lead to dielectric breakdown in solids. The mechanisms which seem to be applicable to the damage observed on the PRIZ are referred to as intrinsic (avalanche) breakdown and discharge breakdown.

Intrinsic, or avalanche, breakdown is electronic in character. Davisson, paraphrasing von Hippel, describes this mechanism as follows:

> The essential mechanism [of intrinsic breakdown] is the creation of directed electron avalanches which are formed by impact ionization of the lattice atoms by electrons which are accelerated by the applied field. Before the electrons can be accelerated, however, they must gain more energy from the field than they lose in exciting or interacting with the longitudinal polar modes of lattice vibration. . . . Once an avalanche of sufficient size has formed, the part of the crystal within the avalanche trail becomes molten due to the local high temperature involved and forms a conducting path of plasma which carries the potential applied to the crystal along the avalanche channel forming a so-called space-charge electrode inside the crystal. The applied voltage is thus brought to the tip of the path. . . . The path will be oriented [with respect to the crystallographic structure] if the electrons experience less friction in some directions than in other, since ionization will occur first in the favourable directions and will thus extend the plasma path in preferred directions (5:68).

Whitehead states, "Behind electron avalanche, is left a channel containing a number of ionized atoms or lattice points. . . . Conduction along the channel may cause permanent damage, perhaps by a process of ionic detachment analogous to melting" (17:107). Referring to the preferred path directions, he reported that they appeared to be in the direction "in which the loss of energy to the lattice from a conduction electron is least in relation to the gain of energy from the field" (17:104). He further stated that breakdown was somehow related

to the effects of mechanical stress and macroscopic defects (17:107).

Discharge breakdown is aptly described by J. C. Anderson. He explains that, since it is difficult to produce a completely homogeneous dielectric, there may be voids in the material, of various shapes and sizes, which contain gas.

> The permittivity of the gas occluded in a cavity will generally be less than that of the surrounding dielectric medium so that, for a given electric stress in the material, the stress in the cavity will be greater to an extent determined by the ratio of permittivity, and by the shape of the cavity (1:113).

(Also, structural defects at certain lattice sites could result in a preferential thermal activity at those sites.)

Anderson then describes the effects of discharge breakdown in polythene. The inside surface of the cavity is subjected to an erosion. Since the energy released by the discharge can instantaneously raise surface temperature of the cavity by hundreds of degrees, this erosion may be thermal in nature. A further increase in electric stress, from the value at which discharge occured, will increase the rate of erosion, with the discharges becoming more concentrated and forming deeper pits (1:117). Anderson also describes fine channels, or paths, in conjuction with the pits, due to discharge breakdown.

> As the discharges continue, the pits attain a critical [depth], after which fine channels propagate from them through the remaining material, causing failure. The mechanism is that the energy liberated increases with the length of the channel over which the discharge occurs. Thus the critical depth of pit is reached when the liberated energy is sufficient to promote rapid destruction of the material. The fineness of the channel is accounted for by the high electric stress which will exist around the fine tip of the breakdown channel. The stress can easily reach the intrinsic breakdown value at the top of a very fine channel (1:117).

Breakdown Paths

Davisson describes several types of breakdown paths, two of which are of significant interest for this report: surface breakdown paths and partial-breakdown paths. Actually, surface breakdown paths are merely partial-breakdown paths which lie on the free surface. "They are observed under the microscope as fine scratches or traces on the surface" (5:62).

Partial-breakdown paths, which can terminate within the material are usually produced by d.c. or pulsed voltages. These paths are hollow channels of small, circular cross-section. A group of partial-breakdown paths, which lie along equivalent crystallographic directions, is called a configuration. Different configurations are possible, but all have a common symmetry for a given crystal, called the breakdown pattern (5:61).

BSO Crystal Damage

The preceding descriptions of breakdown damage apply to dielectrics. However, damage induced on PRIZ devices during this research project (pits, striation, and cracks) bares a striking resemblance to dielectric breakdown.

Under scrutiny with a microscope, the pits showed evidence of high temperatures (see figure 5.1). The bottom of the pits were smooth and rounded, as if a melting had occured. This feature is reminiscent of the pits caused by discharge breakdown, as described by Anderson. Like the discharge-induced pits, the write-beam-induced pits on the BSO crystal increased in concentration and in depth with higher irradiances and voltages.

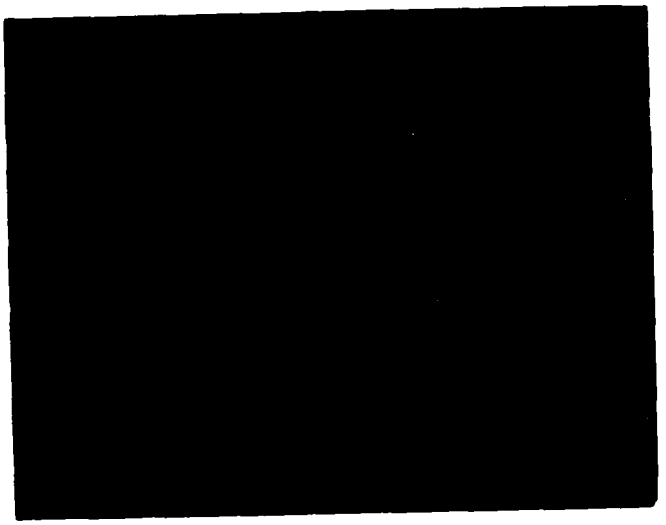

Figure 5.1. Sample of Pit Damage - Crystal #4
(Transmitted light @ 320x).

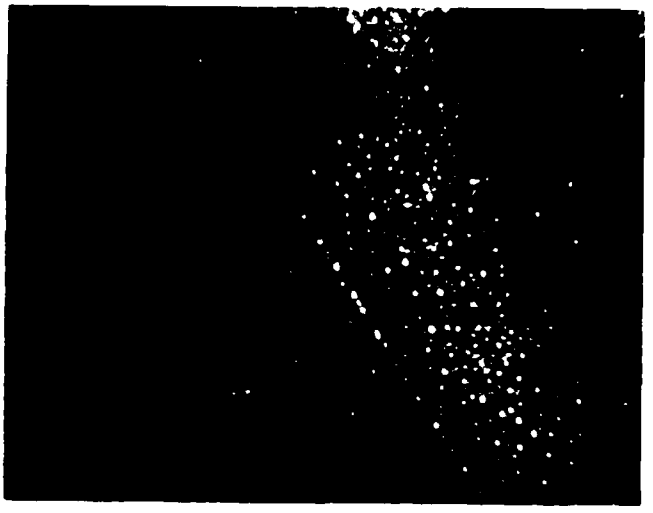

Figure 5.2. Another Sample of Pit Damage - Crystal #4
(Dark-field reflected light @ 320x).

Another similarity is the fine channels emanating from both, previously referred to as striae on the BSO (see figures 5.1 & 5.2). The striation seems to fit both Davisson's description of surface breakdown paths, and Anderson's description of fine channels, emanating from discharge pits. (Recall that in operation of the PRIZ device, there are transverse fields, as well as the longitudinal field, which could drive the discharge paths in transverse directions.) Also, the striae, or surface breakdown paths, display symmetric structure, as predicted by breakdown theory. This structure is what Davisson called the "breakdown pattern".

The larger cubic-corner structure, or propellor patterns, on the BSO crystal, which appeared to be cracks, may be partial-breakdown paths, due to intrinsic, or avalanche, breakdown (see figure 5.3).

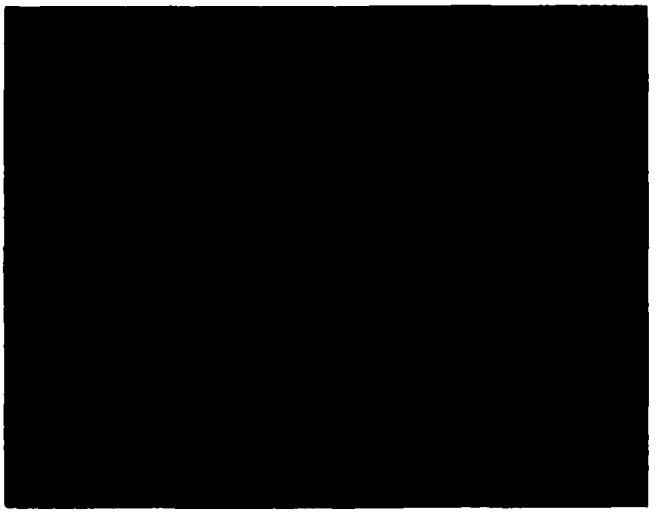

Figure 5.3. Sample of Crack Damage - Crystal #4
(Transmitted light @ 320x).

The "cracks", or paths, display a width which was originally assumed to be due to the crack being nonvertical in some places, i.e. a cross-sectional view would resemble a slash (/). No such angle was visible, however, when the cross-section of cracks were observed, i.e. the cracks were observed to be perpendicular to the surface. Therefore, it is possible that the paths were indeed of circular cross-section. Breaking the crystal could have crimped the path at the crystal's edge, leading to the appearance of a crack. On the other hand, partial-breakdown paths in BSO may occur in the form of crack-like channels rather than circular cross-sectional channels.

The fact that these "intrinsic breakdown" paths emanate from "discharge breakdown" pits, corresponds to Anderson's statement regarding the fine channels which emanate from the pits: "The stress can easily reach the intrinsic breakdown value at the top of a very fine channel." In other words, discharge breakdown could cause the pits and surface breakdown paths (striae), and then, in some cases, intrinsic breakdown induces partial-breakdown paths at the highly stressed tips of the surface breakdown paths.

The fact that intrinsic breakdown occurs on only one side of a crystal, while discharge breakdown occurs on either, requires an explanation. Schwuttke, in describing physical surface damage associated with shaping operations on silicon, may have provided one. He reported that operations such as sawing, grinding, and lapping introduces micro-cracks into silicon, and that the "crack tips represent stress centers . . . [which] are not plastically relieved at room temperatures" (13:564). "Mechanical damage on silicon surfaces

has significant influence on minority carrier lifetime and surface recombination velocities of carriers" (13:562). This, in turn, would influence the conductivity and, hence, the possibility of breakdown.

Similar surface damage, if present on the BSO crystal, could be directly linked to damage susceptibility. The pits induced on the surface could correspond to the presence of micro-cracks. This would explain why damage could not be induced in all locations; in locations where micro-cracks did not exist, damage did not occur.

The restriction of crack damage to only one side of a crystal could be the result of the polishing performed by the manufacturer. (This is not to say that a particular manufacturer has performed poorly, since devices from two manufacturers, were involved, but that the polishing technique, in general, may be faulty.) After a wafer of BSO crystal has been sliced from the boule, or ingot, it is manually polished on one side until that side is "smooth". In reality, the surface is not microscopically smooth due to the micro-cracks. The opposite surface of the crystal is then polished to achieve smoothness and the prescribed thickness, and to ensure that the two surfaces are completely parallel. The later is the most difficult to achieve, and the surface may be repolished several times before it is completely parallel to the first surface. By that time, the second surface has been polished more than the first, removing more of the micro-cracks, i.e. it is microscopically smoother than the first surface.

On the more polished side, the surface has far fewer surface defects, thus, resulting in fewer discharge breakdown pits. However, since this surface has fewer micro-cracks, conductivity will be in-

creased by two mechanisms: first, by influencing the carrier lifetimes and surface recombination velocities of carriers, and second, by improving surface contact with the electrode. This improvement in conductivity would enhance the chances of intrinsic, or avalanche, breakdown occuring at the tips of the surface breakdown paths (which, along with the pits, could be caused by discharge breakdown on either side of the crystal). Thus, the more polished surface is more susceptible to intrinsic breakdown at the few locations where discharge breakdown has occured, while the less polished side is more susceptible to discharge breakdown, and relatively immune to intrinsic breakdown.

All of this, of course, is merely hypothesis. It is uncertain whether dielectric breakdown theory is completely applicable to BSO, or whether the effects of shaping silicon can apply. Still, it is quite possible that the damages observed on the PRIZ device were the results of dielectric breakdown, both intrinsic and discharge, and that nothing more mysterious than the crystal polishing technique determined what type of breakdown occured where. (Also, the piezoelectric effect may have contributed to damage, through mechanical stress.)

VI. Partial Verification of Damage Model

Mechanical preparation of a crystal, e.g. cutting, lapping, and grinding, causes surface disorder; however, the degree of disorder on the crystals used in this research was unknown. In order to establish that disorder was present and to approximate the density of that disorder, chemical etching (see Section IV) was performed on a virgin crystal, i.e. one on which electrodes had never been deposited. An additional goal was to verify that the disorder on the two surfaces differed, as predicted in Section V.

Before etching, there was no noticeable difference between the two surfaces, with or without a microscope. After etching, even without the aid of a microscope, one surface was visibly dull and rough, while the other surface was smooth and shiney. At magnifications of 320x, disorder was found on both surfaces of the virgin crystal. The density of disorder differed roughly by a factor of four between the two surfaces (compare figures 6.1 and 6.2). On the smooth, shiney surface, the density of surface disorder sites was approximately 8500 per mm^2, while on the dull, rough surface, the density was approximately 30000 per mm^2.

As hypothesized in Section V, the dull, rough side would correspond to the surface which is susceptible to striation and dense pit damage (compare figures 6.2 and 5.1), while the smooth, shiney side would correspond to the surface susceptible to crack damage and sparse pit damage.

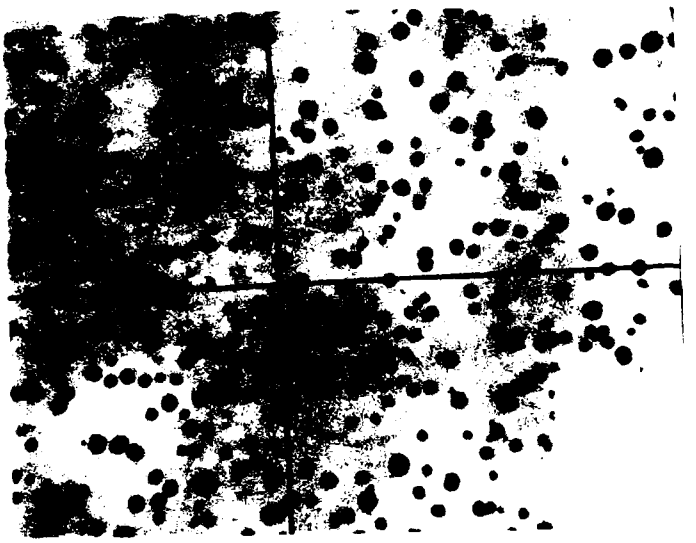

Figure 6.1. Smooth/Shiney Surface after 13 Second Etch - Crystal #5 (Transmitted light @ 320x).

Figure 6.2. Dull/Rough Surface after 13 Second Etch - Crystal #5 (Transmitted light @ 320x).

VII. Summary

In the course of this research project, a great deal of information was uncovered concerning the damage susceptibility of the PRIZ. Although several questions were answered, new questions arose, leaving room for further research.

Conclusions

The PRIZ device proved to be quite susceptible to write-beam-induced damage. The results of this project show that even at the lower end (1000 to 1400 V) of the operating range recommended by Shields, and at relatively moderate write-beam irradiances (326 $\pm$ 20 $\mu W/cm^2$), minor damage to the crystal could, and did, occur. These lower voltages, however, do not lead to optimum performance of the device. At higher voltages (1400 to 2000 V), crystal damage was much more severe. In fact, when the voltage was maintained at 2000 V, minor damage was shown to occur at very low irradiances ($\sim$ 90 $\mu W/cm^2$). However, damage at lower irradiances occurred only after considerable exposure (20 to 30 seconds) of the write-beam to a given location. Naturally, damage was more severe and occurred more quickly at both high voltages (2000 V) and high irradiances ($>$ 300 $\mu W/cm^2$).

Electrode degradation and crystal damage were observed. Crystal damage occurred in the form of pits, striation, and cracks on and just under the surface, to a depth on the order of that of the high-field region. Pits, striation, and cracks all displayed a symmetric pattern which resembled the corner of a cube. This pattern was always oriented

in the same direction, indicating that it corresponded to the crystallographic directions. The striation was overlapping patterns similar to the propellor pattern crack damage, and may, in fact, have been less severe manifestions of the same type of damage. In every case, the damage occurred on the side of the negative electrode, near the high-field region. The negative electrode was applied to both surfaces of a crystal and pit damage was found to be induceable on either side. On one surface, pits were found in dense patches and were accompanied by striation. On the other surface, pits were few and scattered, and accompanied by crack damage.

Chemically etching a virgin crystal revealed that the two larger surfaces of a crystal contained surface disorder, caused by the mechanical preparation of the surfaces. The degree of disorder was greater on one surface by a factor of 4. This could explain the difference in damage type (or severity) between the two surfaces. Upon careful examination of crystals used by previous AFIT researchers, similar damage was found, which had previously elluded detection.

Recommendations

There are several experiments which could be performed to gain a better understanding of the exact mechanisms behind write-beam-induced damage, and the influence of that damage on the operability of the device in practical applications. If the influence is severe, attempts should be made to reduce the device's susceptibility to damage.

Examination of a BSO crystal surface with electron diffraction might prove valuable. Perhaps damage could be directly linked to

defects in the crystal, and the nature of those defects identified.

Of considerable value, would be a more detailed study of damage threshold levels. In this study, the irradiance was first held fixed (at ~ 300 $\mu W/cm^2$), while the E-field voltage was varied (1000 to 2000 V). Then the voltage was held fixed (at 2000 V), while the irradiance of the write-beam was varied (~ 100 to 13000 $\mu W/cm^2$). This represents only a small subset of the possible combinations of values. For example, what damage occurs at 1400 V and 1000 $\mu W/cm^2$, or at 1800 V and 100 $\mu W/cm^2$)? Furthermore, the ranges studied were divided into large increments for this study due to time factors. A tabulated survey of damage, in terms of E-field voltage versus write-beam irradiance, would assist future users of the PRIZ in selecting parameters which would least likely cause damage. The voltage should range from 1000 to 2000 V in increments of 100 V, while the write-beam irradiance might range from 100 to 4000 $\mu W/cm^2$ in increments of 100 $\mu W/cm^2$.

Once such studies have been performed, similar studies should be performed using more realistic write-beam illumination. It should be understood that, in practical applications, the PRIZ would probably not have a laser write-beam focused down on it to a small spot size. Normal applications would entail illuminating the PRIZ with some image of spatially varying irradiance. Additionally, the effect of such damage on the operation of the PRIZ should be examined.

Finally, attempts to reduce damage susceptibility should be considered. Annealing processes, on the mechanically prepared surfaces, should reduce the influence of surface disorder on damage occurrence.

Also, chemical preparation of the crystal surfaces, or combinations of chemical and mechanical preparation, should reduce this influence.

Obviously, if damage can easily be induced on the PRIZ during practical applications, and if the damage seriously degrades the operation of the device, then the PRIZ is not suited for those applications.

Appendix: Previously Reported Damage

Conical Fracture

Shields reported two types of damage (both found on Shields' crystal #S1): one to the crystal and another to the electrodes. The crystal damage was in the form of a conical fracture very similar to the effect of "a BB going through a plate glass window" (see figure A.1). The fracture started at the front, or negative, surface as a small (~ 0.1 mm diameter) hole and flared out to an exit hole nearly 20 times larger. Shields attributed the fracture to "dielectric breakdown of the BSO due to the high current density caused by the laser and high field." The field voltage was set at 1800 volts, while the write-beam irradiance was 500 mW/cm² (13:51-52). Nilius did not observe crystal damage.

Chromium Migration

Shields described the electrode damage as "dendritic trails .... written on the back of the crystal" (see figure A.2). He attributed the damage to "migration of the chromium electrode material to a high field area." The field voltage was set at 2000 volts, while the write-beam irradiance was 500 μW/cm² (13:53). Nilius did observe this electrode damage (7:46-47).

Figure A.1. Conical Fracture - Shields' Crystal #S1
(Transmitted light @ 35x).

Figure A.2. Chromium Migration - Shields' Crystal #S1
(Transmitted light @ 200x).

Bibliography

1. Anderson, J. C. Dielectrics. New York: Reinhold Publishing Corporation, 1964.

2. Casasent, D. et al. "Soviet PRIZ Spatial Light Modulator," Applied Optics, 20 (18): 3090-3092 (September 1981).

3. Casasent, D. et al. "Test and Evaluation of the Soviet PROM and PRIZ Spatial Light Modulators," Applied Optics, 20 (24): 4215-4220 (December 1981).

4. Casasent, David et al. "Applications of the PRIZ Light Modulator," Applied Optics, 21 (21): 3846-3854 (November 1982).

5. Davisson, J. W. "Directional Breakdown Effects in Crystals," Progress in Dielectrics, Volume 1, edited by J. B. Birks and J. H. Schulman. New York: John Wiley & Sons Inc., 1959.

6. Iwasa, Tatsuru. "Chemical Etching and Fabrication of Ridge Waveguides on BiGeO Single Crystals," Journal of Applied Physics, 47 (6): 2746-2748 (June 1976).

7. Nilius, Mark E. Laboratory research notebook for MS Thesis. Air Force Institute of Technology (AU), Wright-Patterson AFB OH, (August 1985 - October 1985).

8. Nilius, Mark E. Measurement and Analysis of the Memory Capabilities of a Conducting PRIZ. MS Thesis GEO-85D-3. School of Engineering, Air Force Institute of Technology (AU), Wright-Patterson AFB OH, (December 1985).

9. Nilius, Mark E. and Theodore E. Luke. Memory and Dynamic Imaging in a Conducting PRIZ. Report. School of Engineering, Air Force Institute of Technology (AU), Wright-Patterson AFB OH, (December 1985).

10. O'Dwyer, J. J. The Theory of Dielectric Breakdown of Solids. Oxford: Clarendon Press, 1964.

11. Petrov, M. P. Current Trends in Optics. Proceeding. (1981).

12. Petrov, M. P. et al. "The PRIZ Image Converter and Its Use in Optical Data Processing Systems," Soviet Physics Technical Physics, 26 (7): 816-821 (July 1981).

13. Schwuttke, G. H. "Pre- and Post-Annealing of Mechanical Damage in Silicon Wafers," Silicon Material Preparation and Economical Wafering Methods, edited by Ralph Lutwack and Andrew Morrison. Park Ridge NJ: Noyes Publications, 1984.

14. Shields, Duncan M. Construction and Analysis of a PRIZ Spatial Light Modulator Exhibiting Dynamic Image Selection. MS Thesis GEO-84D-4. School of Engineering, Air Force Institute of Technology (AU), Wright-Patterson AFB OH, (December 1984).

15. Shields, Duncan M. and Theodore E. Luke. "Operation of a Conducting PRIZ," Optics Communications, 55 (6): 391-392 (October 1985).

16. Stratton, R. "The Theory of Dielectric Breakdown in Solids," Progress in Dielectrics, Volume 3, edited by J. B. Birks and J. H. Schulman. New York: John Wiley & Sons Inc., 1961.

17. Whitehead, S. Dielectric Breakdown of Solids. Oxford: Clarendon Press, 1951.

Vita

First Lieutenant Danny L. Anderson was born on 8 September 1958, in Aurora, Colorado. The son of a career Air Force officer, he travelled extensively throughout his childhood. He graduated from high school in Montgomery, Alabama, in 1976. He earned his Bachelor of Science degree in Physics at Brigham Young University. Upon graduation, in December 1982, he received a commission in the USAF through the ROTC. His first active duty assignment was at HQ Space Command, Peterson AFB, CO. He served as a Missile Warning Systems Acquisitions Officer in the Missile Warning Directorate, DCS Plans. In May 1985, he reported to the School of Engineering, Air Force Institute of Technology, as a Master of Science degree candidate, in Engineering Physics. He is married and has two daughters.

Permanent address: 1023 N. Kingswood Rd.
Kaysville, Utah 84037

UNCLASSIFIED

SECURITY CLASSIFICATION OF THIS PAGE

REPORT DOCUMENTATION PAGE

Form Approved OMB No. 0704-0188

1a. REPORT SECURITY CLASSIFICATION: UNCLASSIFIED	1b. RESTRICTIVE MARKINGS
2a. SECURITY CLASSIFICATION AUTHORITY	3. DISTRIBUTION/AVAILABILITY OF REPORT: Approved for public release; distribution unlimited.
2b. DECLASSIFICATION/DOWNGRADING SCHEDULE	
4. PERFORMING ORGANIZATION REPORT NUMBER(S): AFIT/GEP/ENP/86D-1	5. MONITORING ORGANIZATION REPORT NUMBER(S)
6a. NAME OF PERFORMING ORGANIZATION: School of Engineering; 6b. OFFICE SYMBOL (If applicable): AFIT/ENP	7a. NAME OF MONITORING ORGANIZATION
6c. ADDRESS (City, State, and ZIP Code): Air Force Institute of Technology, Wright-Patterson AFB, OH 45433	7b. ADDRESS (City, State, and ZIP Code)
8a. NAME OF FUNDING/SPONSORING ORGANIZATION; 8b. OFFICE SYMBOL (If applicable)	9. PROCUREMENT INSTRUMENT IDENTIFICATION NUMBER
8c. ADDRESS (City, State, and ZIP Code)	10. SOURCE OF FUNDING NUMBERS: PROGRAM ELEMENT NO. / PROJECT NO. / TASK NO / WORK UNIT ACCESSION NO.

11. TITLE (Include Security Classification)

ANALYSIS OF WRITE-BEAM-INDUCED DAMAGE ON THE CONDUCTING PRIZ (Unclas.)

12. PERSONAL AUTHOR(S)

Danny L. Anderson, B.S., 1ST LT, USAF

13a. TYPE OF REPORT	13b. TIME COVERED	14. DATE OF REPORT (Year, Month, Day)	15. PAGE COUNT
MS Thesis	FROM _____ TO _____	1986 December	62

16. SUPPLEMENTARY NOTATION

17. COSATI CODES			18. SUBJECT TERMS (Continue on reverse if necessary and identify by block number)
FIELD	GROUP	SUB-GROUP	PRIZ, Conducting PRIZ, Damage, BSO, Spatial Light Modulator, Directional Filtering
20	06		

19. ABSTRACT (Continue on reverse if necessary and identify by block number)

Thesis Chairman: Dr. Theodore E. Luke

Approved for public release: IAW AFR 190-1

7 April 87

The susceptibility of the conducting PRIZ to write-beam-induced damage was studied. Using a HeCd laser as a write-beam, damage was intentionally induced on PRIZ devices. Careful examination of the devices revealed essentially four types of damage: "electrode damage", "pit damage", "striation", and "crack damage". Striation may have been a pattern of overlapping less severe crack damage. (Continued on back)

20. DISTRIBUTION/AVAILABILITY OF ABSTRACT	21. ABSTRACT SECURITY CLASSIFICATION
☒ UNCLASSIFIED/UNLIMITED ☐ SAME AS RPT ☐ DTIC USERS	UNCLASSIFIED

22a. NAME OF RESPONSIBLE INDIVIDUAL	22b. TELEPHONE (Include Area Code)	22c. OFFICE SYMBOL
Dr. Theodore E. Luke	513-225-2012	AFIT/ENP

DD Form 1473, JUN 86 *Previous editions are obsolete.*

SECURITY CLASSIFICATION OF THIS PAGE

UNCLASSIFIED

(Continued from block 19)

The write-beam irradiance and applied E-field strength were varied in search of damage thresholds, and analysis was performed to discover the location and nature of the damage. Electrode damage was in the form of either evaporation or migration.

Pit damage, striation, and crack damage were related: all occurred in the "high-field" region of the PRIZ, i.e. near the negative surface; all displayed a symmetric structure resembling the corner of a cube (pits displayed this structure only after chemical etching); and, although striation and cracks did not always appear with pit damage, pits always accompanied striation and crack damage.

On one surface of a crystal, dense patches of pits and striation were induced, while on the other surface, crack damage and fewer pits resulted. This was found to be due to a difference in the surface imperfections caused by the mechanical preparation of the crystals.

Devices used in earlier AFIT research, by Duncan Shields and Mark Nilius, were examined and found to have similar damage. This damage had previously eluded detection.

END

5-87

DTIC